Displacement Currents Associated with the Insertion of Alzheimer Disease Amyloid β-Peptide into Planar Bilayer Membranes

J. Vargas,* J. M. Alarcón,* and E. Rojas*†

*Institute of Biomedical Sciences, Faculty of Medicine, University of Chile, Santiago, Chile, †Laboratory of Biochemistry and Cell Biology, National Institute of Diabetes and Digestive and Kidney Diseases, National Institutes of Health, Bethesda, Maryland 20892 USA and †Sansum Medical Research Institute, Santa Barbara, CA 93105 USA

ABSTRACT The role of endogenous amyloid β-peptides as causal factors of neurodegenerative diseases is largely unknown. We have previously reported that interactions between Alzheimer's disease AβP[1–40] peptide in solution and planar bilayer membranes made from anionic phospholipids lead to the formation of cation-selective channels. We now find and report here that the spontaneous insertion of free AβP[1–40] across the bilayer can be detected as an increase in bilayer capacity. To this end we recorded the displacement currents across planar bilayers (50 mM KCl on both sides) in response to sudden displacements of the membrane potential, from −300 to 300 mV in 20-mV increments. To monitor the AβP[1–40]-specific displacement currents, we added AβP[1–40] (1–5 μM) to the solution on either side of the membrane and noted that the direction of the displacement current depended on the side with AβP[1–40]. The size of the AβP[1–40]-specific charge displaced during a pulse was always equal to the charge returning to the original configuration after the pulse, suggesting that the dipole molecules are confined to the membrane. As a rule, the steady-state distribution of the AβP[1–40]-specific charges within the bilayer could be fit by a Boltzmann distribution. The potential at which the charges were found to be equally distributed (V_o) were ~ −135 mV (peptide added to the solution in the compartment electrically connected to earth) and 135 mV (peptide added to the solution connected to the input of the amplifier). The AβP[1–40]-specific transfer of charge reached a maximum value (Q_{max}) when the electrical potential of the side containing the amyloid β-protein was taken to either −300 or 300 mV. For a circular membrane of 25-μm radius (~2000 μm^2), the total AβP[1–40]-specific charge Q_{max} was estimated as 55 fC, corresponding to some 170 e.c./μm^2. Regardless of the side selected for the addition of AβP[1–40], at V_o the charge displaced underwent an *e*-fold change for a ~27-mV change in potential. The effective valence (*a*) of the AβP[1–40] dipole (i.e., the actual valence *Z* multiplied by the fraction of the electric field χ acting on the dipole) varied from 1 to 2 electronic charges. We also tested, with negative results, the amyloid peptide with the reverse sequence (AβP[40–1]). These data demonstrate that AβP[1–40] molecules can span the low dielectric domain of the bilayer, exposing charged residues (D_1, E_3, R_5, H_6, D_7, E_{11}, H_{13}, and H_{14}) to the electric field. Thus the AβP[1–40] molecules in solution must spontaneously acquire suitable conformations (β-pleated sheet) allowing specific interactions with charged phospholipids. Interestingly, the domain from residues 676 to 704 in the APP_{751} is homologous with the consensus sequence for lipid binding found in other membrane proteins regulated by anionic phospholipids.

INTRODUCTION

Alzheimer's disease (AD) is a chronic dementia characterized by the presence of amyloid plaques in the brain (Selkoe, 1991). The principal component of these plaques (Masters et al., 1985) is a 39–42-residue peptide termed amyloid β-protein (Hardy and Higgins, 1992; Haass and Selkoe, 1993; Haass et al., 1993a,b; Selkoe, 1996), which is a proteolytic product of the widely distributed amyloid precursor glycoprotein (APP_{751}), defined by a locus on chromosome 21 (Goldgaber et al., 1987; Neve et al., 1990; Tanzi et al., 1987). In particular, AβP[1–40] has been linked to the neurotoxic principle causing neuronal death in the disease, although the mechanism has remained elusive (Matson et al., 1992; Kowall et al., 1992; Malouf, 1992; Yankner, 1992). Thus the principal aim of this work was to study the molecular interactions between amyloid β-peptides with planar lipid bilayers, a useful cell membrane model.

We have recently shown that AβP[1–40] in solution can form cation-selective channels across artificial (Arispe et al., 1993a,b, 1994) or natural bilayer membranes (Kawahara et al., 1997). Because AβP[1–40] corresponds to the amyloid precursor protein APP_{751} sequence, from 653 to 695, comprising portions of extracellular and membrane-spanning domains, we proposed that the channel properties could be the underlying cause of amyloid neurotoxicity (Arispe et al., 1994).

Previous studies of channel incorporation into phospholipid bilayers, including porin (Gallucci et al., 1996; Bainbridge et al., 1998), amphotericin B (Fujii et al., 1997), and nisin, a member of the antibiotic family (Giffard et al., 1996), have shown that it is possible to monitor the insertion of the molecules forming pores by following the changes in bilayer capacitance and resistance by means of a dual sinusoidal (1 and 1000 Hz) current method. On the other hand, it has been shown that changes in the bilayer solution environment can induce measurable changes in membrane capacity (Chanturiya and Nikoloshina, 1994).

Received for publication 22 January 1999 and in final form 15 May 2000.

This paper was presented to the Biophysical Society in abstract form (1997).

Address reprint requests to Dr. Eduardo E. Rojas, Sansum Medical Research Institute, 2219 Bath Street, Santa Barbara, CA 93105. E-mail: erojas@sansum.org.

0006-3495/00/08/934/11 $2.00

To study the interactions between free AβP[1–40] molecules and the phospholipids in the bilayer we measured the changes in membrane capacitance associated with the incorporation of peptides into the bilayer. The underlying hypothesis was that the insertion of peptides into the low dielectric region of the bilayer will expose AβP[1–40] charges to the electric field. Thus application of sudden changes in potential should, at least in principle, displace mobile peptide charges, and this charge displacement in turn could be detected with conventional electrophysiological techniques. This technique has been used before in single nerve fibers (Cole and Curtis, 1939; Armstrong and Bezanilla, 1974; Nonner et al., 1975; Keynes and Rojas, 1974, 1976), in planar bilayer membranes (Alvarez and Latorre, 1978), and in bilayers formed at the tip of a patch pipette (Rojas and Pollard, 1987).

We found and report here that the insertion of AβP[1–40] but not AβP[40–1] molecules occurs only if the peptide interacts with anionic membrane phospholipids and only while it is undergoing transitions within a restricted set of conformations. Our observation that AβP[1–40] interacts only with bilayer membranes formed from anionic but not neutral lipids provides support for our idea that amyloid β-peptide susceptibility occurs when acidic phospholipids are transposed to the outer face of the membrane. The anionic phospholipid asymmetry, which is actively maintained by flippase, a specific cell membrane ATPase, diminishes the probability of amyloid β-peptide insertion into the cell membrane.

MATERIALS AND METHODS

Artificial bilayer membranes

The methods used here have previously been described (Wonderlin et al., 1990; Arispe et al., 1993a). In brief, the experimental chamber consisted of two Plexiglas blocks (3 × 1.5 × 1 cm) with two cylindrical compartments each (1 cm^3 and 0.4 cm^3). The compartments (1 cm^3) were separated by a thin (10-μm) Teflon film with a small circular hole at the center. The hole was made by means of an electric arc between two platinum needles on either side of the Teflon film. The area of the hole at the center of the Teflon film separating the two pools of the chamber was measured with a binocular microscope, before and after the bilayer was formed. Spreading the lipid solution across this hole (as a rule, 50 μm in diameter) always left a toroidal lipid rim (~2–5 μm thick).

To form a bilayer on this hole, we used a 1:1 mixture of synthetic palmitoyloleoylphosphatidylethanolamine (POPE) and synthetic palmitoyloleoylphosphatidylserine (PS) (Avanti Polar Lipids, Birmingham, AL) dissolved in decane (~50 mg/ml). The compartment electrically connected to the input probe of the voltage-clamp amplifier will be referred to as the p-pool. The other compartment, which was electrically connected to earth, will be referred to as the e-pool. A plastic spatula was used to form planar bilayers by spreading the phospholipid mixture, dissolved in decane, on the hole. Two Ag/AgCl pellet electrodes were immersed in cylindrical pools (0.4 cm^3) filled with 50 mM KCl on either side of the bilayer pools. Bridges of 2% agar–50 mM KCl salt glass were used to electrically connect the electrode minipools (0.4 cm^3) with the pools (1 cm^3) on either side of the bilayer.

For the experiments reported here we used AβP[1–40] and AβP[40–1] peptides obtained from Bachem (Torrance, CA). The peptides were dissolved in water (Milli-Q) at a concentration of 100 μM. For each experiment we added an aliquot of the amyloid β-peptide water solution to one compartment of the chamber (final concentration ≤ 5 μM).

Data acquisition and analysis

The electrical potential of the solution in the p-pool is referenced to that in the e-pool. Positive charges moving from the p-pool to the e-pool across the bilayer during a positive voltage pulse represent positive current. Single sweep displacement currents across the bilayer were recorded with an EPC-7 patch-clamp amplifier (List Electronic, Darmstadt, Germany). The performance of the feedback amplifier was routinely tested for linearity and frequency response. For this task, we used either a dummy circuit (provided by the manufacturer of the EPC-7 amplifier), consisting of a 10-GΩ resistor in parallel with a 10-pF capacitor and a 5-kΩ resistor in series, or a circuit representing a typical planar bilayer membrane used here. We also tested the performance of the instruments required to acquire the records on-line. These include an eight-pole Bessel band-pass filter (902 LPF; Frequency Devices) and a patch-clamp amplifier–computer interface that was equipped with 12-bit AD and DA converters (Tl-1 DMA; Axon Instruments). For this task we used a calibration dummy made up of a 200-GΩ (± 1%) resistor (R_m) in parallel with a 10-pF (± 0.1%) capacitor (C_m) and a 5-kΩ resistor in series (R_s). The error introduced by the signal acquisition system was less than ±5%.To minimize the membrane conductance due to leakage, we used a symmetrical solution system of low ionic strength (in mM: 50 KCl, 5 KHepes, pH 7.2–7.4).

To acquire and record the displacement currents, we used a digital system and pClamp 6 software provided by Axon Instruments (Foster City, CA). Pulse protocols were generated by a TL-1 DMA interface equipped with a 12-bit DAC and a 12-bit ADC converter, running synchronously at 250 kHz and controlled by a board (Scientific Solutions) installed in a 486 PC. Permanent records of the current transients were made using the Clampex subroutine of the pClamp 6 data acquisition software package (Axon Instruments). During a standard experimental protocol a family of current transients in response to rectangular voltage clamp pulses was digitized at 25 kHz. Each family consisted of a series of current records in response to rectangular voltage pulses of increasing amplitude in the range from −300 to 300 mV. When necessary, to form an average of a current transient, each pulse was applied 30 times at a repetition rate of 1 s^{-1}. Off-line analysis was carried out using both the subroutine Clampfit of the Pclamp 6 software package and the software Origin 4.1 (Microcal Software, North Hampton, MA).

RESULTS

AβP[1–40]-specific asymmetrical displacement currents

To measure the minute peptide-specific charge movements across the bilayer, we had to set the amplifier gain at either 50 or 100 mV/pA. For this reason, the initial current surge after sudden changes in membrane potential always saturated the amplifier; recovery from saturation occurred in less than 50 μs.

Each superimposed truncated transient shown in Fig. 1 represents the current in response to a rectangular pulse taking the potential of the p-pool solution from 0 to ± 160 mV. Under control conditions (no AβP[1–40] added), the "on" as well as the "off" transients are symmetrical (Fig. 1 *A*). In contrast, ~5 min after the addition of AβP[1–40] to the p-pool (final concentration 1.35 μM), an additional

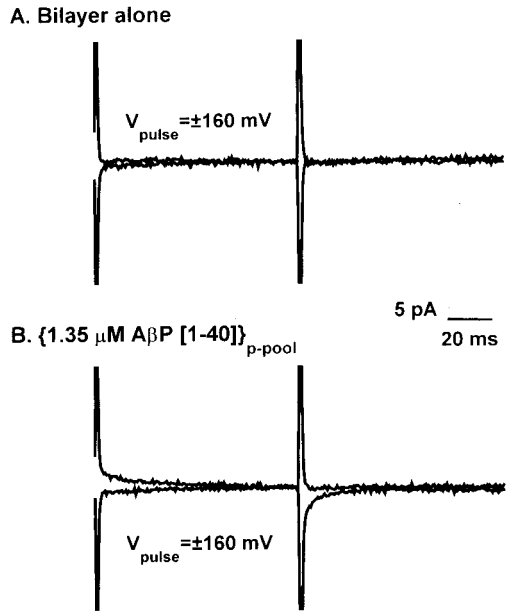

FIGURE 1 Displacement currents across a bilayer formed from anionic phospholipids. (*A*) Symmetrical displacement currents across the bilayer alone in response to rectangular pulses of alternating polarity (±160 mV). Bilayer resistance: 266 GΩ; bilayer capacitance: 7.2 pF (see Fig. 2). (*B*) Asymmetrical displacement currents across the same bilayer ~5 min after the addition of 1.35 μM AβP[1–40] to the p-pool.

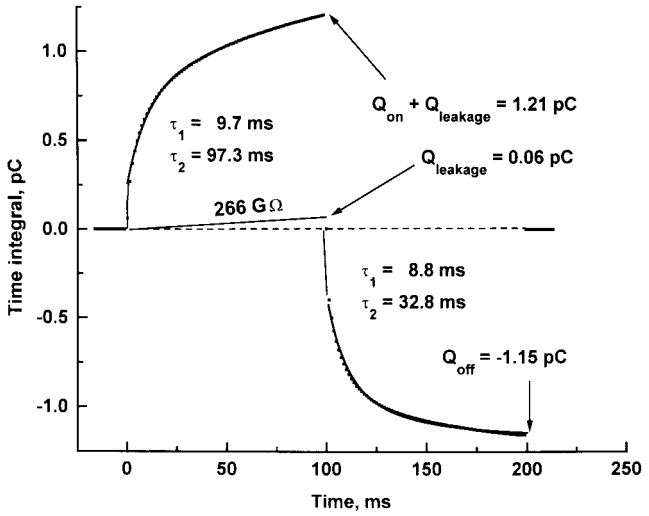

FIGURE 2 Time integral of the displacement currents across the anionic phospholipid bilayer alone. Filled square symbols represent one of every three data points taken from the time integral of the displacement current record. The charge movement was elicited by a 100-ms duration rectangular pulse, taking the membrane potential from 0 to 160 mV (Fig. 1 *A*). Line through the black squares represents the least-squares fit of a double-exponential function plus a linear function. The time constants from the fit are shown under (*left*) or over (*right*) the corresponding record. Straight line represents the time integral of a pedestal of leakage current. Bilayer resistance: ~266 GΩ (0.16 V/0.6 pA); bilayer capacitance: ~7.2 pF (1.15 pC/0.16 V).

component appeared (Fig. 1 *B*). This AβP[1–40]-dependent component of the current is expressed only during and after the application of positive voltage pulses and is totally absent from the records for negative pulses. This result suggests a highly polarized insertion of the AβP[1–40] peptide. The presence of displacement current transients exhibiting AβP[1–40]-specific asymmetry (Fig. 1 *B*) suggests that the direction of the AβP[1–40]-specific displacement currents is determined by the pool to which the peptide is added.

Quantitative evaluation of both capacitance and resistance of the bilayer alone was obtained from the analysis of the charge displacement in the absence of peptide. Q_{on}, the charge displaced during a pulse (see Fig. 1 *A*), was estimated as the time integral of the current surge in response to a 160-mV pulse. As depicted in Fig. 2, the time course of $Q_{on}(t)$ can be described as the sum of two exponentially rising functions (resulting from the presence of different populations of charges available for displacement) plus a linear component (resulting from the integration of a pedestal of leakage current).

Fig. 2 shows the time integral of the current transient depicted in Fig. 1 *A*, elicited by a rectangular voltage pulse that takes the membrane potential across the bilayer from its holding value of 0 mV to 160 mV. Because the record was acquired before the application of AβP[1–40] to the p-pool, the time integral (in pC) of the current transients (in pA) during and after a rectangular voltage pulse allowed us to estimate both the capacity (C_m) and the leakage resistance of the bilayer (R_m). While the value of the bilayer capacity estimated from Q_{off} requires no assumptions, the calculation of the bilayer resistance assumes that charge movements are confined to the bilayer. Therefore, the charge displaced during the pulse, Q_{on}, should be equal to the charge after the pulse, i.e., $-Q_{off}$. However, as depicted in Fig. 2, Q_{on} (1.21 pC) is greater than $-Q_{off}$ (1.15 pC). We attributed the difference to the contribution of the leakage current to the charge. Therefore, $Q_{on} + Q_{off}$ should be equal to $Q_{leakage}$, i.e., 0.06 pC. Then the leakage current during the pulse $I_{leakage}$ is calculated as 0.6 pA (= 0.06 pC/0.1 s). The bilayer leak resistance, $R_{leakage}$, is calculated as 266 GΩ (= 0.16 V/0.6 pA). If we compare the cell membrane capacity, i.e., 1 $\mu F/cm^2$ (Cole and Curtis, 1939), with that of a typical planar lipid bilayer membrane used here (measured area of 2000 μm^2), the bilayer capacitance should be about three times what we measured. However, it should not be forgotten that the cell membrane is endowed with a set of intrinsic proteins spanning the membrane bilayer, including ion channels, receptors, and transporters. These proteins might make a contribution with mobile charged domains.

It should also be noted here that the time integrals of the displacement currents, during and after the pulse, could be fit with the sum of two exponential functions. Furthermore, only the slow relaxation time constant varied from 97.3 ms (at 160 mV) to 32.8 ms (at 0 mV). After the rectangular

pulse, the change in time constant from 9.7 ms to 8.8 ms was not statistically significant.

The time integral of the current transients across the bilayer alone (Fig. 2) revealed that the size of the charge transferred during the pulse (Q_{on}) is slightly greater than that after the pulse (Q_{off}). We also noted that in both the absence (Fig. 2) and presence of AβP[1–40], the charge $Q_{on}(t)$ is made up of one linear and two exponential components (see Fig. 2). In the presence of AβP[1–40] the sizes of the nonlinear and linear components are augmented. In contrast, regardless of the presence of AβP[1–40], owing to the fact that the bilayer is exposed to a symmetrical solution system and the holding potential is kept at 0 mV, in most of the experiments the linear component is absent from the time integral of the displacement current after the pulse $Q_{off}(t)$. The linear component of the time integral during the pulse shown in Fig. 2 (*solid line*) corresponds to a leakage of ~0.06 pA. Therefore, in the absence of amyloid β-peptide, the resistance of the bilayer (area ~2000 μm^2) was ~266 GΩ.

Rectification of AβP[1–40]-specific displacement currents suggests that insertion of the Aβ-peptide is vectorial in character

We have already shown that when the peptide AβP[1–40] is present in the p-pool and the bilayer potential is held at 0 mV, the net AβP[1–40]-specific displacement current in response to a positive pulse is in the positive direction (Fig. 1 *B*).

Fig. 3 *A* shows that, at a holding potential of 0 mV, when the amyloid β-protein is added to the solution in the p-pool, the polarity of the displacement current during the pulse is positive. In contrast, the addition of the peptide to the e-pool generated a negative-going asymmetrical displacement current during the pulse (Fig. 3 *B*). Taken together, the data in Figs. 1 and 3 demonstrate that the polarity of the amyloid-specific displacement current depends on the side of the bilayer exposed to the amyloid β-protein. An important mechanistic conclusion can be drawn from these results, namely that insertion of the AβP[1–40] molecule is vectorial in character and that the peptide remains highly polarized in the membrane.

To test whether peptide-bilayer interactions depend on specific structural conformations of the AβP[1–40] in water solution and not on the presence of the structural residues, we repeated these experiments, using the peptide with the reverse sequence, i.e., AβP[40–1], with negative results. That is, peptide-specific displacement currents could not be detected with the peptide AβP[40–1] in place of AβP[1–40]. Indeed, as shown in Fig. 4 (*left*), two pairs of superimposed records of the tail currents evoked by ±190 mV pulses, one pair in the absence and the other 5 min after the addition of 5 μM AβP[40–1], remained unmodified. The right panel shows the corresponding Q_{off} values as a function of the membrane potential during the pulses. It is apparent that the size of the AβP[40–1]-specific charge movement is negligible.

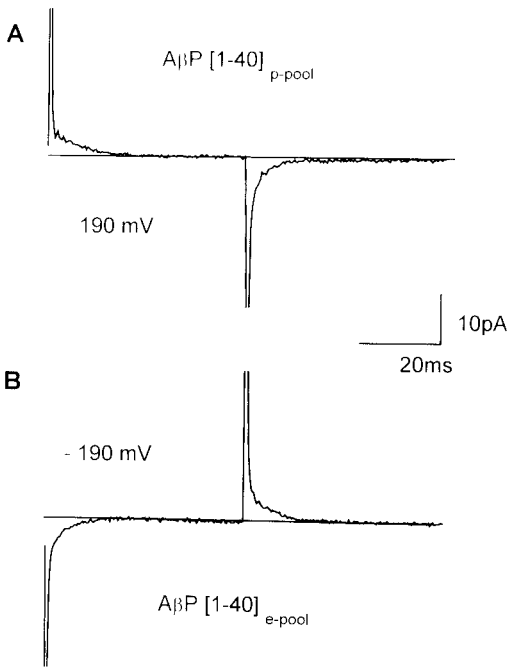

FIGURE 3 AβP[1–40]-specific asymmetrical displacement current polarity is determined from the side of the pool with the amyloid peptide. Each trace represents the average of 30 records. The membrane potential during each pulse is indicated next to the corresponding record. The peptide was added to the p-pool for the record in *A* and to the e-pool for the record in *B*.

AβP[1–40]-specific charge movements are confined to the bilayer

If the components of the asymmetrical current are to be identified with the displacement of charged domains within the AβP[1–40] peptide inserted in the bilayer, then the total transfer of charge during rectangular voltage pulses (Q_{on}) should be exactly balanced by the transfer of mobile charge after the pulse in the other direction (Q_{off}), when the potential returns to the holding level. However, like natural cellular membranes, artificial phospholipid bilayers are not perfect isolators and are endowed with a leakage pathway. To test this equality, we evaluated both Q_{on} and Q_{off} from the time integral during and after rectangular pulses of increasing amplitude. Fig. 5 depicts the linear relationship between $-Q_{off}$ (*ordinate*) and Q_{on} (*abscissa*) for the displacement of AβP[1–40]-specific charges, during and after the pulses. It should be mentioned here that the data in Fig. 5 were acquired during an experiment in which AβP[1–40] was present in the p-pool. Furthermore, all Q_{on} values were corrected for $Q_{leakage}$ as described in Fig. 2. The straight line

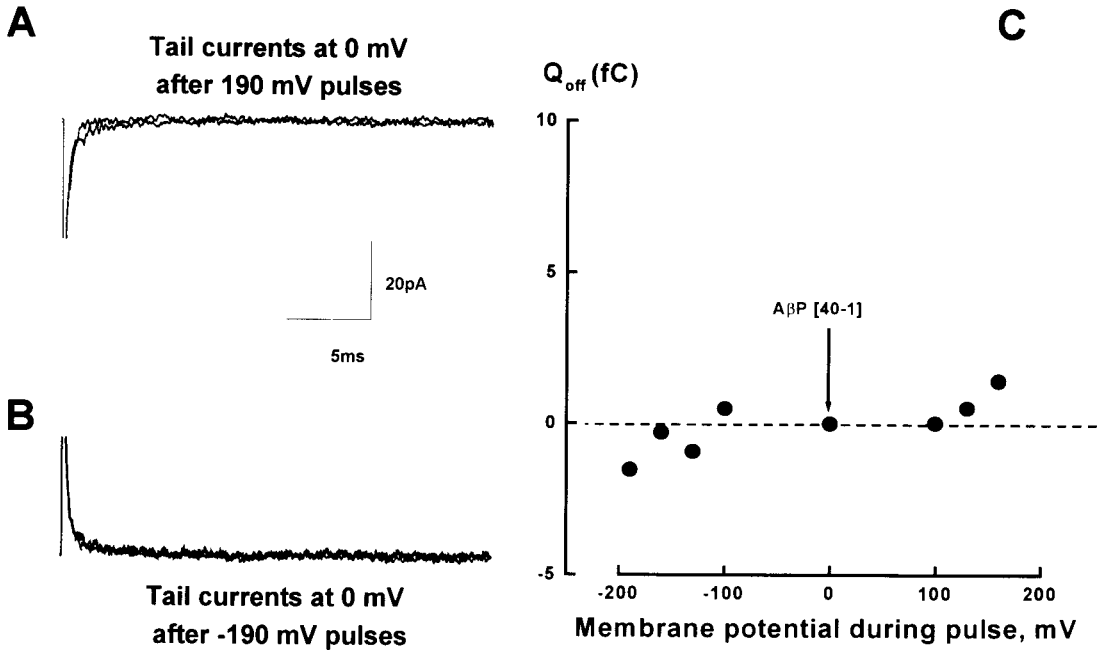

FIGURE 4 Exposure of anionic phospholipid planar bilayers to the peptide AβP[40–1] with the reverse sequence does not induce asymmetrical displacement currents. Superimposed displacement tail currents shown on the left were acquired in both the absence and presence of 5 μM AβP[40–1]. The graph on the right represents the AβP[40–1]-specific charge Q_{off} displaced at the end of positive and negative pulses of increasing amplitude. This was estimated as the difference Q_{off} in the absence minus Q_{off} in the presence of the peptide.

represents a least-squares linear regression fit, the slope of which was found not to be significantly different from unity.

Voltage dependence of the steady-state distribution of the AβP[1–40]-specific mobile charges

In the absence of an electrical potential gradient across the bilayer the charges on the AβP[1–40] residues will acquire a particular distribution across the membrane (for details on the model used here see Rojas, 1976). A sudden change in potential will cause a rearrangement of the mobile charges that continues in time until a new equilibrium distribution of the charges is achieved. Shown in Fig. 6 are the normalized values of Q_{on}/Q_{min} plotted against the membrane potential from two different experiments. For the data depicted in Fig. 6, the bilayer was exposed to AβP[1–40] from either the e-pool (Fig. 6 *A*) or the p-pool (Fig. 6 *B*). The sigmoid

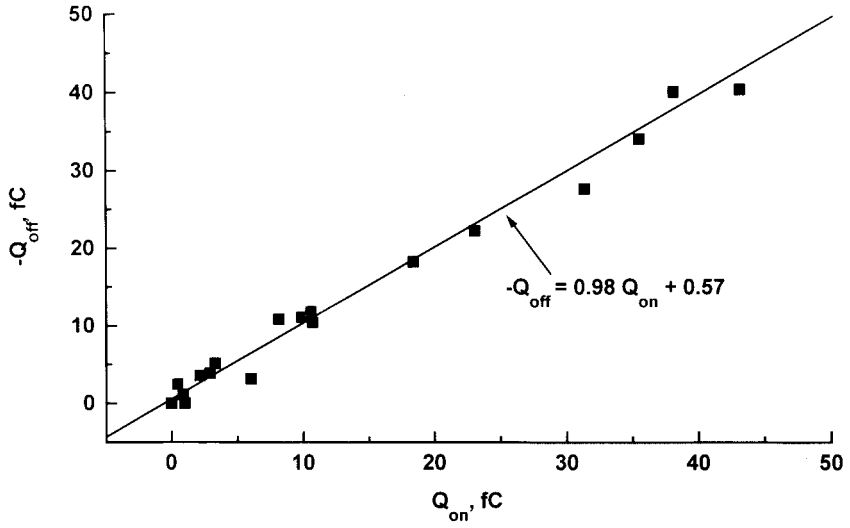

FIGURE 5 Charge displaced after the pulse ($-Q_{off}$) as a function of the charge displaced during the pulse (Q_{on}). Each symbol represents the net AβP[1–40]-specific displacement current Q_{on}, elicited by rectangular voltage pulses of increasing amplitude, from 60 to 200 mV. The peptide was added to the p-pool. Straight line represents a linear least-squares fit of the data points. Slope = 0.98, intercept 0.57 fC.

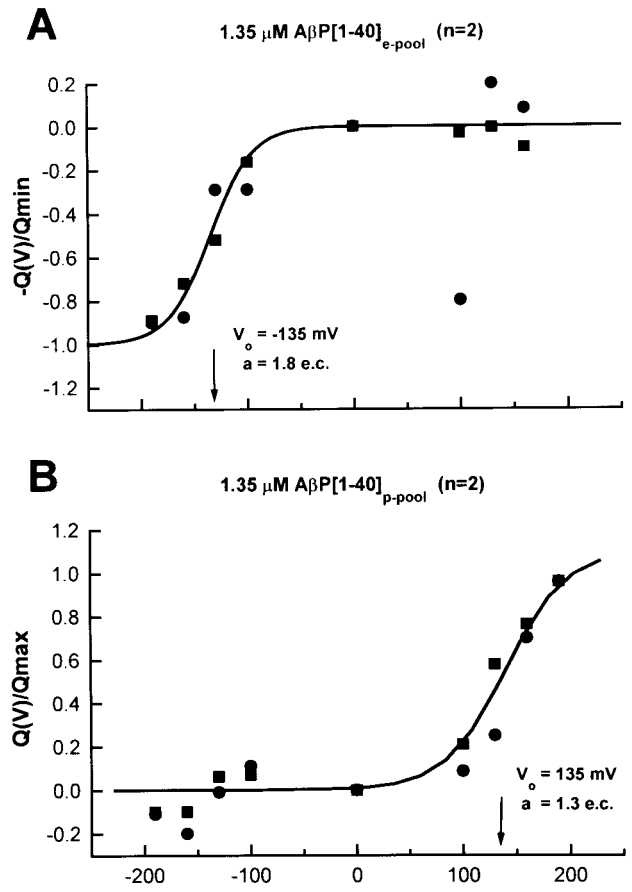

FIGURE 6 Steady-state distribution of the dipole charges. (*A*) AβP[1–40] added to the e-pool. The vertical axis represents normalized $Q(V)/Q_{min}$, where $Q(V)$ represents the AβP[1–40]-specific charge displaced during the pulse. Q_{min} represents the maximum negative charge displaced. The horizontal axis is the same for the two panels. The sigmoidal curve represents the least-squares fit of the Boltzmann function to the data. The parameters of the fit are given above the horizontal axis (each symbol represents a different experiment). (*B*) AβP[1–40] added to the p-pool. $Q(V)/Q_{max}$ normalized charge displaced during the pulse.

curves represent a least-squares fit of the following Boltzmann-type function:

$$Q_{on}(V)/Q_{on,max} = 1/\{1 + \exp^{a(V-V_o)/kT}\}$$

where a ($= \chi z$) represents the effective valence (z) of the mobile charge multiplied by the fraction (χ) of the electric field across the bilayer acting on the charge. The Boltzmann constant k times the absolute room temperature T is taken to be 24.2 meV. Only one set of values was used for the least-squares sigmoid function fit (Fig. 6, *filled circles*). It is immediately apparent that, provided the holding potential is kept at zero between the pulses, the midpoint potential V_o for the distribution depends on the side chosen for amyloid β-protein presentation. Indeed, the average V_o is ~−135 mV for amyloid additions to the e-pool (Fig. 6 *A*) and is ~135 mV for amyloid additions to the p-pool (Fig. 6 *B*). Interestingly, the effective valence is rather similar in the two instances, 1.8 and 1.3, respectively. The meaning of these results is that in both systems, at V_o changes in membrane potential from 20 to 27 mV will displace ~63% of $Q_{on,max}$. Taken together, these data provide persuasive support for the polarized insertion of the AβP[1–40] peptides into the bilayer.

The data presented so far suggest that the equilibrium distribution of AβP[1–40] peptide charges depends on the potential gradient across the bilayer. To further test this mechanism we studied the effects of the holding potential on the tail currents after voltage pulses (Fig. 7).

Fig. 7 shows the effects of varying the holding potential on AβP[1–40]-specific tail currents after the application of rectangular 160-mV pulses of alternating polarity. Fig. 7 *A* depicts the superimposed tail currents in response to ±160-mV pulses recorded at a holding potential of 0 mV,

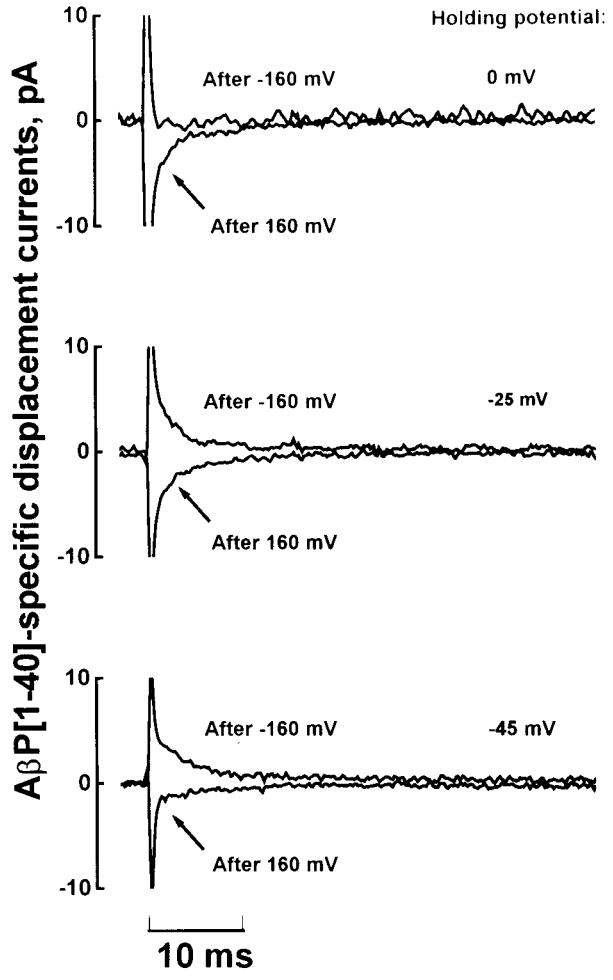

FIGURE 7 Effects of holding potential on the distribution of charges. (*A–C*) Two superimposed tail currents after 160-mV symmetrical rectangular pulses of alternating polarity. AβP[1–40] peptide (1.35 μM) was added to the p-pool. Data acquisition started 5 min after the peptide was added (*A*). For changes in holding potential (*B* and *C*), data acquisition was begun immediately after the change.

from a bilayer exposed to AβP[1–40] added to the p-pool. Fig. 7, *B* and *C*, shows the changes in tail currents induced by holding the membrane at negative potentials of −25 and −40 mV. It should be noted that at a holding potential equal to −25 mV, the tail currents after ±160-mV pulses are nearly the mirror image of each other. The similarity in amplitude and kinetics suggests that the AβP[1–40] dipoles are equally distributed.

Nonpolarized interactions between AβP[1–40] and planar bilayer membranes formed from a mixture of 50% phosphatidylcholine and 50% cholesterol

We have already established that AβP[1–40] does not form cation channels across planar bilayer membranes formed from mixtures of the neutral lipids phosphatidylcholine (PC) and cholesterol (Chol) (Arispe et al., 1993b). Our structural model of the AβP[1–40]-cation channel (Durell et al., 1994) is based on two hypotheses: first, charged peptides interact spontaneously with anionic phospholipids in the bilayer, and second, polarized insertion of the peptides forms a pore spanning the membrane. To further elucidate the nature of peptide-lipid interactions, we prepared planar bilayer membranes from PC-Chol mixtures and repeated, with negative results, the studies describe above.

Fig. 8 shows typical records of displacement currents from an experiment designed to compare bilayer resistance and capacity before and after the addition of 1.35 μM AβP[1–40] to the e-pool in a PC-Chol bilayer. It should be noted that to avoid saturation of the amplifier during the current surges, the gain was reduced to 1 V/nA (Fig. 8, *A* and *B*). From the analysis of the corresponding time integrals (Fig. 8, *C* and *D*), we estimated that the leakage resistance of the PC-Chol bilayer increased from 80 GΩ, in the absence of AβP[1–40], to 133 GΩ in its presence. Although we have no explanation for this result, it is possible that nonpolarized insertion of the AβP[1–40] peptide into the neutral hydrophobic environment provided by PC

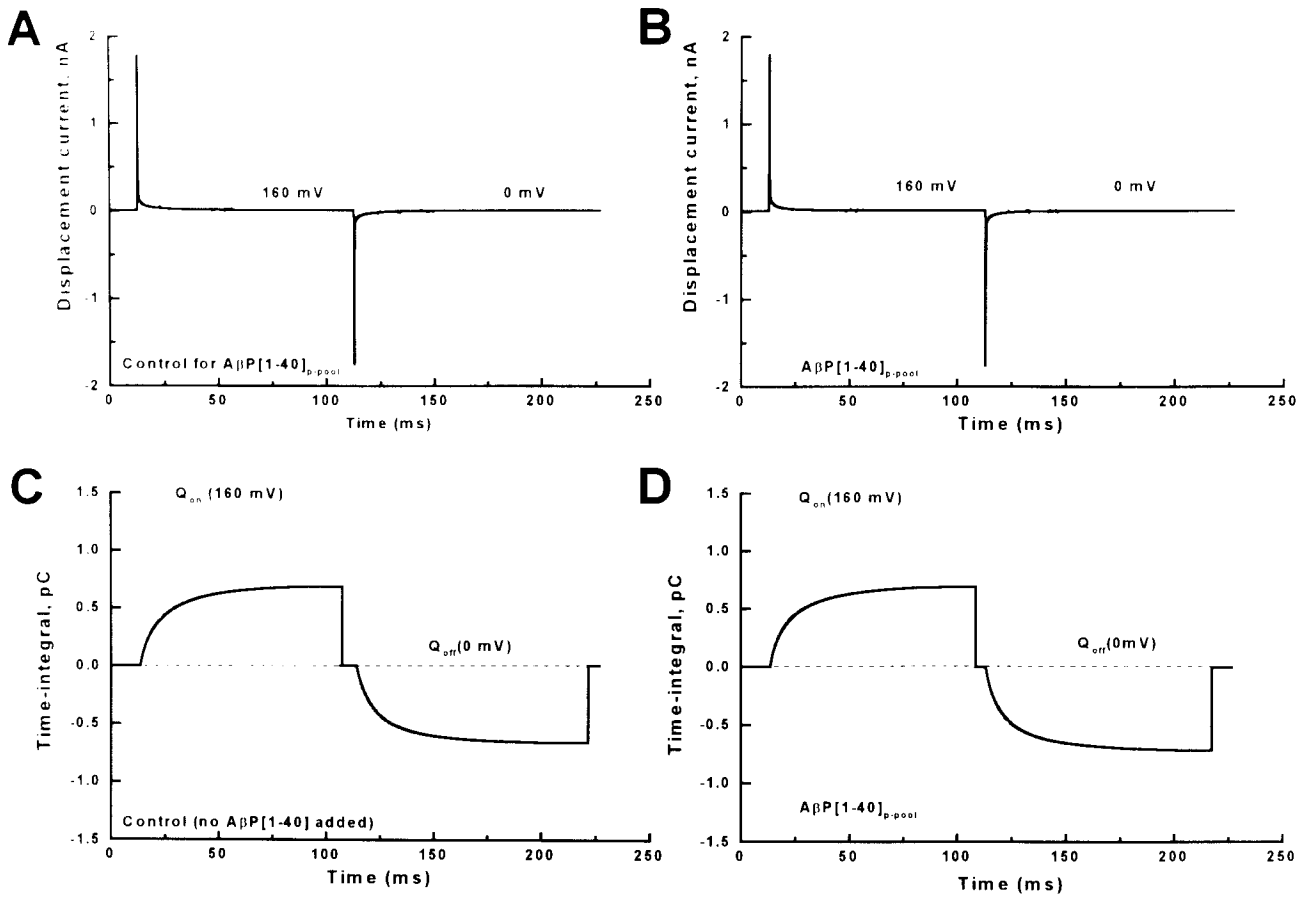

FIGURE 8 Free AβP[1–40] peptides in solution do not induce asymmetrical displacement currents in bilayer membranes formed from 50% PC and 50% cholesterol. (*A* and *B*) Displacement current transients across the bilayer alone (*A*) and in the presence of AβP[1–40] added to the e-pool (*B*). (*C* and *D*) Time integrals of the displacement current transients across the bilayer alone (*C*) and in the presence of AβP[1–40] added to the e-pool (*D*). Bilayer resistance and capacitance: 80 GΩ and 5.8 pF in the absence of AβP[1–40]; 133 GΩ and 6.7 pF in the presence of AβP[1–40].

and Chol may improve the molecular packing in the bilayer, decreasing its fluidity and its leak current.

A comparison of the charge displaced in response to rectangular pulses (from −200 to 200 mV) across bilayers formed from 50% PC and 50% Chol, before (Fig. 9, *empty circles*) and after the exposure to AβP[1–40] (Fig. 9, *filled circles*), revealed that the charge displaced is unaffected by the addition of the amyloid peptide to either the p-pool (Fig. 9 *A*) or the e-pool (Fig. 9 *B*). It should be noted that the charge Q_{off} displaced across bilayers made of PC/Chol mixtures is linearly related to the membrane potential across the bilayer, both in the absence of the peptide (Fig. 9, *empty circles*) and in the presence of 1.35 mM AβP[1–40] in the e-pool (Fig. 9, *filled circles*). This result clearly shows that the size of the displacement currents across a bilayer alone remains unchanged upon exposure to AβP[1–40]. The absence of AβP[1–40]-specific charge displacement (Fig. 9, *empty squares*) makes it immediately apparent that the AβP[1–40] peptide was unable to insert itself into bilayers made of 50% PC and 50% Chol.

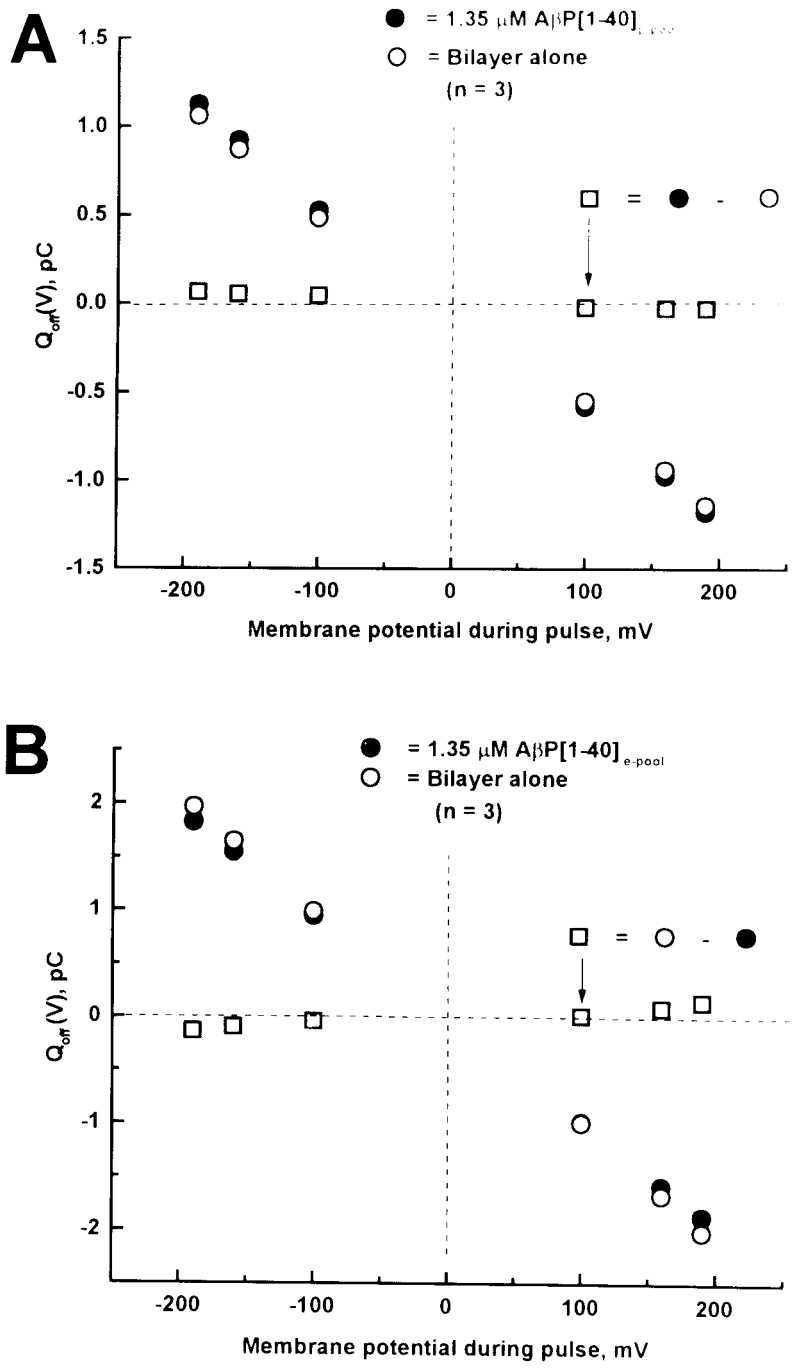

FIGURE 9 Linear charge displacement across PC/Chol bilayers is not affected by AβP[1–40]. (*A*) Q_{off} as a function of membrane potential. ○, Bilayer alone; ●, bilayer exposed to 1.35 μM AβP[1–40] from the p-pool. Average capacitance: 6.1 pF. (*B*) Q_{off} as a function of membrane potential. ○, Bilayer alone; ●, bilayer exposed to 1.35 μM AβP[1–40] from the e-pool. In *A* and *B* open squares represent the net AβP[1–40]-specific charge displaced. Average capacitance: 10.8 pF.

In conclusion, we found no evidence to support the idea that AβP[1–40] interacted with PC-Chol bilayers by the same mechanism proposed by us to explain the spontaneous insertion of the peptide into bilayers formed from anionic phospholipids.

Experiments designed to study the dependence of AβP[1–40] insertion across planar bilayer membranes made from mixtures of cholesterol and the acidic phospholipid PS revealed that the incorporation of AβP[1–40] into the bilayers depended on the fraction PS/Chol. As illustrated in Fig. 10, peptide insertion requires the presence of at least 5% PS in the bilayer, achieving a maximum peptide insertion across bilayers made from ~95% PS plus 5% Chol. Thus it is clear that Chol prevents the incorporation of AβP[1–40] into PS bilayers. Furthermore, as illustrated in Fig. 10, the normalized data ($Q_{off}/Q_{off,\ max}$), as a function of the percentage of PS in the bilayer, could be fit with a sigmoidal function. Interestingly, the presence of 26% PS in the cholesterol bilayer allows the insertion of 50% of the maximum admissible level of inserted AβP[1–40] peptides.

DISCUSSION

The main contribution of this study is to provide, for the first time, a molecular mechanism to explain the interactions between Alzheimer's β-amyloid peptide and cellular membranes, possibly leading to an explanation for AD amyloid β-peptide neurotoxicity.

Polarized insertion of AβP[1–40] into bilayers made from anionic, but not neutral or cationic, phospholipids

The principal aim of this study was to provide a molecular mechanism to explain the neurotoxicity of amyloid β-peptides. We found and report here that free amyloid β-peptides in water solutions can interact with planar bilayer membranes made from anionic, but not from neutral phospholipids. Another important contribution of the present study is the demonstration of the ability of AβP[1–40], proposed by some to be the causal factor of neuronal death in AD, to insert itself across planar anionic phospholipid bilayer membranes. As for the molecular interactions, this study also provides evidence that the AβP[1–40] insertion into anionic planar bilayer membranes is highly polarized.

We also showed here that the lipid composition of the planar bilayer plays a crucial role in amyloid β-peptide–bilayer membrane interactions. We show here that while the amyloid β-peptide spontaneously inserts itself across planar bilayers made from anionic phospholipids to form cation-selective channels, the effect of its interaction with bilayers formed from a mixture of neutral phospholipids, cholesterol and PC, is only to increase membrane resistance. Indeed, with the techniques used here, we failed to detect the vector of AβP[1–40] into PC/Chol membranes. This result is consistent with the idea that the polarized insertion of AβP[1–40] into a planar lipid bilayer is driven by electrochemical interactions between peptides and membranes. Because the carboxyl and the choline group in the polar head of PC form a salt link (Rojas and Tobias, 1965; Santis and Rojas, 1969), it is reasonable to expect a profound decrease in the electrostatic forces between peptide and PC. Finally, it should be mentioned here that the surface pressure-area isotherms of monolayers of PC or cholesterol alone spread at the air-water solution (50 mM KCl, pH 7) interface are not affected by the presence of AβP[1–40] in the solution (Rojas, unpublished observations). These observations imply that AβP[1–40] interactions with neutral bilayers may be inside the hydrophobic domain and that

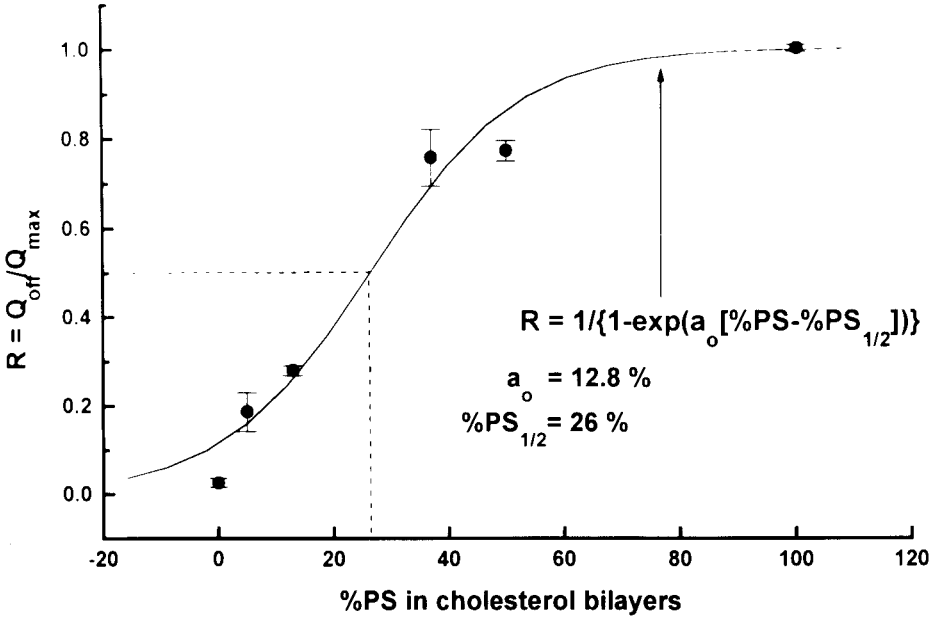

FIGURE 10 AβP[1–40] peptide insertion across planar bilayers formed from Chol and PS mixtures. The vertical axis represents the ratio $Q_{off}/Q_{off,\ max}$ (R). The abscissa represents the PS percentage in the cholesterol bilayers. The membrane was exposed to 1.35 μM AβP[1–40] from the e-pool. Open circles represent the average value of R (n = 3) ± SEM. The sigmoid curve represents a least-squares fit of the function $1/\{1 - \exp(a_o[\%PS - \%PS_{1/2}])\}$ to the experimental data. The parameter a_o represents the slope at the midpoint of the curve (*dashed lines*).

neutral bilayers do not hold the peptide in a polarized conformation.

AD peptides in solution tend to polymerize in saline solutions. For this reason, it has been proposed by some that only the aggregated form of the peptide is neurotoxic. Based on the findings presented here, we propose that free AβP[1–40] peptide in solution is able to insert itself across the bilayer in both artificial and natural membranes. Indeed, we have already shown that AβP[1–40] forms cation-selective, Zn^{2+}-sensitive channels across excised patches from hypothalamic neurons (Kawahara et al., 1997). Because the normal brain is exposed to amyloid peptides, the mechanism proposed here implies that AβP[1–40] damage occurs only in susceptible neurons.

Matson et al. (1992) showed that β-amyloid peptides destabilize calcium homeostasis and render human cortical neurons susceptible to exocitoxicity. Interestingly, we also found and have communicated elsewhere that exposure to either Alzheimer's peptide AβP[1–40] or human pancreatic islet amylin can induce a substantial elevation in cytosolic free-calcium concentration in hypothalamic neurons (Kawahara et al., 2000). Taken together, these data provide further evidence supporting the idea that AβP[1–40] can induce marked increases in $[Ca^{2+}]_i$ resulting from increased Ca^{2+} influx through AβP channels spontaneously formed in the plasma membrane of susceptible GT1–7 neurons. This unregulated Ca^{2+} influx might eventually saturate intracellular Ca^{2+} stores, causing cell death. We propose that the susceptibility of cells to AβP[1–40] damage depends on the acidity of the cell membrane's external aspect.

Cation-channel hypothesis provides a mechanism to explain amyloid toxicity

The data presented here lend strong support to the "amyloid-channel hypothesis" (Arispe et al., 1993a,b, 1994; Durell et al., 1994), which provides a molecular mechanism for cell degeneration in the brain of AD patients. One can extend this concept to explain cell toxicity of other amyloid peptides identified as causal factors in other age-related diseases.

Cholesterol: a potential neuroprotective factor?

It is well established that interactions of protein molecules in solution and lipids in bilayer membranes are modulated by membrane fluidity (Gottfries et al., 1996a,b). Furthermore, cholesterol has been shown to decrease the fluidity of artificial and natural membranes, affecting the ability of antibiotic peptides to form channels (Lundbaek et al., 1996; Fujii et al., 1997; Kawahara et al., 2000). In addition, cholesterol has also been reported to influence the conformation of AβP in membranes in vitro. Coincidentally, human amylin, another member of the amyloid β-peptide family, does not form channels across cholesterol-rich membranes (Mirzabekov et al., 1996). Finally, amyloid AβP[25–35] toxicity tested on PC12 cells was shown to be inhibited by cholesterol (Zhou and Richardson, 1996).

The data presented here show, at a molecular level, that AβP[1–40] in solution inserts itself vectorially across anionic phospholipid (POPE/PS) bilayers, but not across membranes formed from neutral cholesterol or phospholipids (PC) (Figs. 8 and 9). Last, we show that the addition of cholesterol to anionic bilayers diminishes the vectorial insertion of AβP[1–40]. Unpublished data from our laboratory show that the addition of 50% cholesterol into planar bilayer membranes formed from anionic phospholipids decreases the ability of AβP[1–40] peptides to form channels across planar bilayers. We may tentatively conclude that a reduction in AβP[1–40] vectorial insertion inhibits resulting AβP[1–40]-channel activity and supports the notion that the AβP[1–40] channels are formed by clusters of the peptide (Durell et al., 1994). Earlier observations showed that increasing the fraction of cholesterol molecules in the POPE/PS membrane inhibited the formation of channel activity by AβP[1–40] (Arispe et al., 1993a). Furthermore, exposing the extracellular aspect of excised neuronal membrane patches to AβP[1–40] did not induce channel activity, whereas exposing the inner aspect did (Kawahara et al., 1997).

We already know that increasing the fraction of cholesterol molecules in neuronal (Kawahara et al., 1997) and planar lipid bilayer (Arispe et al., 1993a,b) membranes brings about a substantial decrease in the fraction of acidic phospholipids in the membrane, known to be important for AβP[1–40] insertion (Kawahara et al., 1997). In line with this interpretation, we observed that the latency of AβP[1–40] incorporation was almost doubled after the cholesterol treatment (Kawahara et al., 2000). Further support for the "cholesterol protection hypothesis" is provided by studies of apolipoproteins of the E-type, which transports and modulates metabolism of cholesterol (Beffert et al., 1998). Furthermore, it has been reported that the cholesterol content in brains of Alzheimer's patients is lower than in normal subjects (Gottfries et al., 1996a,b). Taking these results together, one might propose that the cholesterol content of neuronal membranes may influence the affinity of the cell membrane for AβP[1–40].

As for the molecular mechanism, it is well established that the peptides used in this study spontaneously acquire β-pleated sheet architecture (Durell et al., 1994; Selkoe, 1996). It is then possible that the essential feature common to all pathogenic channel forming peptides is the β-pleated sheet structure in combination with hydrophobic domains (Carrell and Lomas, 1997).

The authors are grateful to Drs. I. Atwater, N. Arispe, and D. Mears for critical reading of the manuscript.

Supported in part by the Presidential Cathedra 1996 and Fondecyt 1950774 to E. R. and a Ph.D. thesis grant (Fondecyt 2980064) to J. M. A.

REFERENCES

Alvarez, O., and R. Latorre. 1978. Voltage-dependent capacitance in lipid bilayers made from monolayers. *Biophys. J.* 21:1–17.

Arispe, N., H. B. Pollard, and E. Rojas. 1993a. Giant multilevel cation channels formed by Alzheimer disease amyloid beta-protein (AβP-[1–40]) in bilayer membranes. *Proc. Natl. Acad. Sci. USA*. 90: 10573–10577.

Arispe, N., Pollard, H. B., and E. Rojas. 1994. β-amyloid Ca^{2+}-channel hypothesis for neuronal death in Alzheimer disease. *Mol. Cell. Biochem.* 140:119–125.

Arispe, N., E. Rojas, and H. B. Pollard. 1993b. Alzheimer disease amyloid β-protein forms calcium channels in bilayer membranes: blockade by thrometamine and aluminum. *Proc. Natl. Acad. Sci. USA*. 90:567–571.

Armstrong, C. M., and F. Bezanilla. 1974. Charge movement associated with the opening and closing of the activation of the Na channels. *J. Gen. Physiol.* 63:533–552.

Bainbridge, G., Mobasheri, H., Armstrong, G. A., Lea, E. J. A., and J. H. Lakey. 1998. Voltage-gating of *Escherichia coli* porin: a cystine-scanning mutagenesis study of loop 3. *J. Mol. Biol.* 275:171–176.

Beffert, U., M. Danik, P. Krzywkowski, C. Ramassamy, F. Berrada, and J. Poirier. 1998. The neurobiology of apoproteins and their receptors in the CNS and Alzheimer's disease. *Brain. Res. Rev.* 27:119–142.

Carrell, R. W., and D. A. Lomas. 1997. Conformational disease. *Lancet.* 350:134–138.

Chanturiya, A. N., and H. V. Nikoloshina. 1994. Correlation between changes in membrane capacitance induced by changes in ionic environment and the conductance of channels incorporated into bilayer lipid membranes. *J. Membr. Biol.* 137:71–77.

Cole, K., and J. Curtis. 1939. Electrical impedance of the squid giant axon during activity. *J. Gen. Physiol.* 22:649–670.

Durell, S. R., H. R. Guy, N. Arispe, E. Rojas, and H. B. Pollard. 1994. Theoretical models of the ion channel structure of amyloid β-protein. *Biophys. J.* 67:2137–2145.

Fujii, G., J. E. Chang, T. Coley, and B. Steere. 1997. The formation of amphotericin B ion channels in lipid bilayers. *Biochemistry*. 36: 4959–4968.

Gallucci, E., S. Micelly, and G. Monticelli. 1996. Pore formation in lipid bilayer membranes made of phosphatidylinositol and oxidized cholesterol followed by means of alternating current. *Biophys. J.* 71:824–831.

Giffard, C. J., S. Ladha, A. R. Mackie, D. C. Clark, and D. Sanders. 1996. Interaction of nisin with planar lipid bilayers monitored by fluorescence recovery after photobleaching. *J. Membr. Biol.* 151:293–300.

Goldgaber, D., M. I. Lerman, O. W. McBride, U. Saffiotti, and D. C. Gajdusek. 1987. Characterization and chromosomal localization of a cDNA encoding brain amyloid of Alzheimer's disease. *Science.* 235: 877–880.

Gottfries, C. G., B. Jungbjer, I. Karlsson, and L. Svennerholm. 1996a. Reductions in membrane proteins and lipids in basal ganglia of classic Alzheimer disease patients. *Alzheimer Dis. Assoc. Disord.* 10:77–81.

Gottfries, C. G., I. Karlsson, and L. Svennerholm. 1996b. Membrane components separate early-onset Alzheimer's disease from senile dementia of the Alzheimer type. *Int Psychogeriatr.* 8:365–372.

Haass, C., A. Y. Hung, M. G. Schlossmacher, T. Oltersdorf, D. B. Teplow, and D. J. Selkoe. 1993a. Normal cellular processing of the β-amyloid precursor protein results in the secretion of the amyloid β peptide and related molecules. *Ann. N.Y. Acad. Sci.* 695:109–116.

Haass, C., A. Y. Hung, M. G. Schlossmacher, D. B. Teplow, and D. J. Selkoe. 1993b. β-Amyloid peptide and a 3-kDa fragment are derived by distinct cellular mechanisms. *J. Biol. Chem.* 268:3021–3024.

Haass, C., and D. J. Selkoe. 1993. Cellular processing of β-amyloid precursor protein and the genesis of amyloid β-peptide. *Cell.* 75: 1039–1042.

Hardy, J. A., and G. A. Higgins. 1992. Alzheimer's disease: the amyloid cascade hypothesis. *Science.* 256:780–783.

Kawahara, M., Y. Kuroda, N. Arispe, and E. Rojas. 1997. Alzheimer's disease amyloid β-protein forms Zn^{2+}-sensitive channels across excised membrane patches from hypothalamic neurons. *Biophys. J.* 73:67–75.

Kawahara, M., Y. Kuroda, N. Arispe, and E. Rojas. 2000. Alzheimer's β-amyloid, human islet amylin and prion fragment evoke intracellular free-calcium elevations by a common mechanism in hypothalamic neuronal cell-line. *J. Biol. Chem.* 275:14077–14083.

Keynes, R. D., and E. Rojas. 1974. Kinetics and steady-state properties of the charged system controlling sodium conductance in the squid giant axon. *J. Physiol. (Lond.)*. 239:393–434.

Keynes, R. D., and E. Rojas. 1976. The temporal and steady-state relationships between activation of the sodium conductance and movement of the gating particles in the squid giant axon. *J. Physiol. (Lond.)*. 255:157–189.

Kowall, N. C., A. C. McKee, B. A. Yankner, and M. F. Beal. 1992. In vivo neurotoxicity of beta amyloid [β(1–40)] and the β(25–35) fragment. *Neurobiol. Aging.* 13:537–542.

Lundbaek, J. A., P. Birn, J. Girshman, A. J. Hansen, and O. S. Anderson. 1996. Membrane stiffness and channel function. *Biochemistry.* 35: 3825–3830.

Malouf, A. T. 1992. Effect of beta amyloid peptides on neurons in hippocampal slice cultures. *Neurobiol. Aging.* 13:543–551.

Masters, C. L., G. Simms, N. A. Weinman, G. Multhaup, B. L. McDonald, and K. Beyreuther. 1985. Amyloid plaque core protein in Alzheimer disease and Down syndrome. *Proc. Natl. Acad. Sci. USA*. 82: 4245–4249.

Matson, M. P., B. Cheng, D. Davis, K. Bryant, I. Lieberberg, and R. E. Rydel. 1992. β-Amyloid peptides destabilize calcium homeostasis and render human cortical neurons vulnerable to exocytotoxicity. *J. Neurosci.* 12:376–389.

Mirzabekov, T. A., M.-C. Lin, and B. L. Kagan. 1996. Pore formation by the cytotoxic islet amyloid peptide amylin. *J. Biol. Chem.* 271: 1988–1992.

Neve, R. L., L. R. Dawes, B. A. Yankner, L. L. Benowitz, W. Rodriguez, and G. A. Higgins. 1990. Genetics and biology of the Alzheimer amyloid precursor. *Prog. Brain Res.* 86:257–267.

Nonner, W., E. Rojas, and R. Stampfli. 1975. Displacement currents in the node of Ranvier. *Pflugers Arch.* 354:1–18.

Rojas, E. 1976. Gating mechanism for the activation of the sodium conductance in nerve membranes. *Cold Spring Harb. Symp. Quant. Biol.* 40:305–320.

Rojas, E., and H. B. Pollard. 1987. Membrane capacity measurements suggest a calcium-dependent insertion of synexin into phosphatidylserine bilayers. *FEB Lett.* 217:25–31.

Rojas, E., and J. M. Tobias. 1965. Membrane model: association of inorganic cations with phospholipid monolayers. *Biochim. Biophys. Acta.* 94:394–404.

Santis, M., and E. Rojas. 1969. On the chemistry of ion exchange in monomolecular layers of lipids. *Biochim. Biophys. Acta.* 193:319–332.

Selkoe, D. J. 1991. The molecular pathology of Alzheimer's disease. *Neuron.* 6:487–498.

Selkoe, D. J. 1996. Cell biology of the beta-amyloid precursor protein and the genetics of Alzheimer's disease. *Cold Spring Harb. Symp. Quant. Biol.* 61:587–596.

Tanzi, R. E., J. F. Gusella, P. C. Watkins, G. A. P. Bruns, P. St. George-Hyslop, M. L. Van Keuren, D. Patterson, S. Pagan, D. M. Kurnit, and R. L. Neve. 1987. Amyloid β protein gene: cDNA, mRNA distribution, and genetic linkage near the Alzheimer locus. *Science.* 235:880–882.

Wonderlin, W. F., R. J. French, and N. J. Arispe. 1990. Recording and analysis of currents from single ion channels. *In* Neurophysiological Techniques: Basic Methods and Concepts, Vol. 14. A. A. Boulton, G. B. Baker, and C. H. Vanderwolf, editors. Humana Press, Totowa, NJ. 35–142.

Yankner, B. A. 1992. Commentary and perspective on studies of beta amyloid neurotoxicity. *Neurobiol. Aging.* 13:615–616.

Zhou, Y., and J. S. Richardson. 1996. Cholesterol protects PC12 cells from beta-amyloid induced calcium disordering and cytotoxicity. *Neuroreport.* 7:2487–2490.